Simultaneous inhibition of hsp 90 and the proteasome promotes protein ubiquitination, causes endoplasmic reticulum-derived cytosolic vacuolization, and enhances antitumor activity

Edward G. Mimnaugh,[1] Wanping Xu,[1] Michele Vos,[2] Xitong Yuan,[1] Jennifer S. Isaacs,[1] Kheem S. Bisht,[3] David Gius,[3] and Len Neckers[1]

[1]Urologic Oncology Branch, [2]Cell and Cancer Biology Branch, and [3]Radiation Oncology Branch, Center for Cancer Research, National Cancer Institute, NIH, Rockville, Maryland

Abstract

The ansamycin antibiotic, geldanamycin, targets the hsp 90 protein chaperone and promotes ubiquitin-dependent proteasomal degradation of its numerous client proteins. Bortezomib is a specific and potent proteasome inhibitor. Both bortezomib and the geldanamycin analogue, 17-*N*-allylamino-17-demethoxy geldanamycin, are in separate clinical trials as new anticancer drugs. We hypothesized that destabilization of hsp 90 client proteins with geldanamycin, while blocking their degradation with bortezomib, would promote the accumulation of aggregated, ubiquitinated, and potentially cytotoxic proteins. Indeed, geldanamycin plus bortezomib inhibited MCF-7 tumor cell proliferation significantly more than either drug alone. Importantly, while control cells were unaffected, human papillomavirus E6 and E7 transformed fibroblasts were selectively sensitive to geldanamycin plus bortezomib. Geldanamycin alone slightly increased protein ubiquitination, but when geldanamycin was combined with bortezomib, protein ubiquitination was massively increased, beyond the amount stabilized by bortezomib alone. In geldanamycin plus bortezomib-treated cells, ubiquitinated proteins were mostly detergent insoluble, indicating that they were aggregated. Individually, both geldanamycin and bortezomib induced hsp 90, hsp 70, and GRP78 stress proteins, but the drug combination superinduced these chaperones and caused them to become detergent insoluble. Geldanamycin plus bortezomib also induced the formation of abundant, perinuclear vacuoles, which were neither lysosomes nor autophagosomes and did not contain engulfed cytosolic ubiquitin or hsp 70. Fluorescence marker experiments indicated that these vacuoles were endoplasmic reticulum derived and that their formation was prevented by cycloheximide, suggesting a role for protein synthesis in their genesis. These observations support a mechanism whereby the geldanamycin plus bortezomib combination simultaneously disrupts hsp 90 and proteasome function, promotes the accumulation of aggregated, ubiquitinated proteins, and results in enhanced antitumor activity. [Mol Cancer Ther 2004;3(5): 551–66]

Introduction

The benzoquinone ansamycin natural product, geldanamycin, and its modified derivative, 17-*N*-allylamino-17-demethoxy geldanamycin (17-AAG), specifically interact with the NH_2-terminal ATP/ADP binding pocket of hsp 90, inducing a conformational change in the hsp 90 chaperone molecule that destabilizes its numerous chaperoned ''client'' proteins (1–3). Following the binding of ansamycins to hsp 90, its client proteins become ubiquitinated and are rapidly down-regulated via proteasomal degradation (4–7). Among the coterie of hsp 90 clients known to be geldanamycin and 17-AAG sensitive are inappropriately overexpressed and/or mutated proteins that initiate and promote tumor cell growth and survival (for reviews, see Refs. 8–10). Both geldanamycin and 17-AAG have substantial antitumor activity as single agents in preclinical cultured tumor cell and xenograft models (11, 12), but animal toxicity studies revealed that geldanamycin caused dose-limiting hepatotoxicity. Fortunately, 17-AAG was subsequently found to be less hepatotoxic than geldanamycin, and this ansamycin was selected as the first-in-class hsp 90-targeting agent to undergo clinical trials as a potential anticancer drug (13). Phase I results with this drug have been encouraging, and 17-AAG is now undergoing more extensive phase II evaluation.

The regulation of signal transduction, transcriptional activation, cell cycle, and cell survival pathways is dependent on short-lived proteins that are degraded by the ubiquitin-dependent proteasome pathway (14–16). Given that aberrant, mutated, and/or overexpressed versions of these regulatory proteins are frequently involved in neoplasia (*i.e.*, oncoproteins), pharmacological manipulation of the proteasome to interfere with the regulated proteolysis of oncoproteins involved in proliferation and survival pathways might be uniquely damaging to cancer cells (17). Thus, proteasome inhibitors have been shown to effectively arrest the growth of tumor cells in culture, xenografted tumors in animals, and primary cultures of human tumor cells (18, 19). Moreover, at least some tumor cells have been found to be more sensitive to proteasome inhibition than their normal counterparts (20). Ultimately, proteasome inhibition causes cell death by apoptosis (21), although the mechanistic details remain murky and are probably multifactored (22). Even so, the proteasome has been recognized as a potentially

Received 12/2/03; revised 3/1/04; accepted 3/9/04.

Requests for Reprints: Edward G. Mimnaugh, Urologic Oncology Branch, Center for Cancer Research, National Cancer Institute, NIH, 9610 Medical Center Drive, Suite 300, Rockville, MD 20850. Phone: (301) 496-5231; Fax: (301) 402-4422. E-mail: edmim@mail.nih.gov

exploitable molecular target for cancer chemotherapy, and advanced clinical trials of the first reversible proteasome inhibitor, bortezomib (also known as Velcade and PS-341), are under way (23, 24). Preliminary reports indicate that bortezomib has substantial activity against refractory multiple myeloma and non-Hodgkin's lymphoma (25–27). Now poised to move into combinatory trials with conventional chemotherapeutic agents and radiation, bortezomib will be evaluated against various types of refractory and advanced metastatic solid tumors as well as hematological malignancies (28, 29).

Recent investigations into the mechanism of antitumor action of bortezomib have centered on its ability to inhibit activation and nuclear translocation of the nuclear factor-κB (NF-κB) transcription factor (28, 30), an important regulator of cellular stress and activator of an exceptionally large number of genes that confer survival advantage to nascent tumors (31, 32). Bortezomib blocks the proteasome-mediated degradation of NF-κB's inhibitory partner protein, IκB, preventing the NF-κB-dependent transcriptional response (33, 34). However, given the quantity and diversity of known proteasome substrates (35, 36), it seems plausible that other consequences of proteasome inhibition may also contribute to the antitumor activity of bortezomib.

The accumulation of bortezomib-stabilized, misfolded, ubiquitinated, probably nonfunctional, and potentially nonrepairable proteins would be expected to interfere with cell signal transduction, cell cycle checkpoints, protein trafficking, and vital cell survival pathways. We reasoned further that geldanamycin-destabilized hsp 90 client proteins would substantially add to the abundance of misfolded, ubiquitinated proteins that amass in proteasome-inhibited cells. Although, at first glance, the combination of a drug promoting protein degradation with a drug that inhibits protein degradation appears to be antithetical, we demonstrate here that bortezomib plus geldanamycin is an effective antitumor combination *in vitro*. Our data indicate that drug-induced accumulation of insoluble, ubiquitinated proteins in both cytosolic and endoplasmic reticulum (ER) compartments is especially noxious to tumor cells and eventually contributes to their demise.

Materials and Methods

Tumor Cells and Drug Treatments

Mycoplasma-free MCF-7 human breast tumor cells were obtained from the American Type Culture Collection (Manassas, VA) and were maintained in DMEM supplemented with 10% heat-inactivated fetal bovine serum, 2 mM L-glutamine, and 10 mM HEPES (pH 7.5) under standard tissue culture conditions of 5% CO_2 and 37°C. Subconfluent, exponentially growing cells were treated with bortezomib alone (Millennium Pharmaceuticals, Boston, MA), geldanamycin alone (National Cancer Institute, NIH, Bethesda, MD), or combinations of both drugs at several concentrations and for various times. Control MCF-7 cells received equivalent volumes of DMSO solvent [0.05% (v/v)]. The antiproliferative activity was measured in 96-well plates seeded with 2000 MCF-7 cells/well; 24 h later, they were exposed to geldanamycin and bortezomib alone or various combinations of the two drugs. Cell survival was evaluated either 3 or 4 days later by the 3-(4,5-dimethylthiazol-2-yl)-2,5-diphenyltetrazolium bromide spectrophotometric assay (37).

Immortalized NIH 3T3 human fibroblasts transfected and selected with the LXSN empty vector, the human papillomavirus (HPV) 16-E6 (*HPV16-E6*) gene (HFF3/LXSN/16E6), and both *HPV16-E6* and *HPV16-E7* genes (HFF3/LXSN/16E6/E7) were obtained from Dr. Denise Galloway (Fred Hutchinson Cancer Research Center, Seattle, WA; Ref. 38). These cells were grown in DMEM with high glucose containing 10% fetal bovine serum, 100 units/ml penicillin, and 100 μg/ml streptomycin and passaged when they reached 75% confluency. The cytotoxic effects of 17-AAG, bortezomib, or both drugs toward these three cell lines were monitored by clonogenic assay as described previously (39). Briefly, LXSN control, HFF3/LXSN/16E6, and HFF3/LXSN/16E6/E7 cells were seeded at 2×10^5 cells in 10 cm culture dishes and allowed to grow to ~75% confluency before drugs were added to the growth medium in a range of concentrations. Cells were trypsinized 24 h later, counted, diluted, and seeded into six-well tissue culture plates. Colonies formed from surviving cells over 10 days were fixed, stained, and counted. Individual clonogenic assays were performed at multiple dilutions with a total of six observations per data point, and the results were verified twice for a total of three identical replicates.

Other experiments included the addition of cycloheximide (50 μg/ml), the geldanamycin analogues, 17-AAG, WX514, and geldampicin (Developmental Therapeutics Program, National Cancer Institute, NIH), and the hsp 90-targeting agents, radicicol and radicicol oxime (Kyowa Hakko Kogyo, Tokyo, Japan) to cells.

Proteasome Assay

Cells exposed to various concentrations of bortezomib or geldanamycin for 1 h were twice washed with PBS and lysed into TNESV buffer [50 mM Tris-HCl (pH 7.5), 1% NP40 detergent, 2 mM EDTA, 100 mM NaCl, 10 mM sodium orthovanadate] without protease inhibitors, and 20 μl aliquots were assayed for proteasome chymotrypsin activity using the synthetic fluorogenic peptide chymotrypsin substrate, succinyl-Leu-Leu-Val-Tyr-7-amido-4-methylcoumarin (Bachem Bioscience, King of Prussia, PA), exactly as described (40). Preliminary experiments with control and bortezomib-treated cells indicated that reaction rates were linear for at least 2 h. We validated the assay of the inhibition of proteasome activity by bortezomib by replacing it with two other proteasome inhibitors, epoxomicin and lactacystin. Bortezomib and geldanamycin were also added directly to untreated cell lysates just prior to the proteasome assay. For the recovery experiment, cells were exposed to 25 nM bortezomib for 2 h, the drug-containing medium was aspirated, and cells were washed and reincubated in fresh complete medium without bortezomib for various times.

Transfections

In certain experiments, tumor cells were transiently transfected using FuGene 6 (Roche Molecular Biochemicals, Indianapolis, IN) with plasmids expressing the Living Colors ER membrane marker that targets the COOH-terminal Lys-Asp-Glu-Leu retrieval sequence of calreticulin as well as plasma membrane and Golgi markers, all fused to enhanced yellow fluorescent protein (Clontech Laboratories, Inc., Palo Alto, CA). Controls cells were transfected with empty vector DNA or a plasmid vector expressing only unmodified yellow fluorescent protein.

Immunoreagents and Other Chemicals

The antibodies used were rabbit polyclonal anti-ubiquitin (Sigma Chemical Co., St. Louis, MO), mouse monoclonal anti-hsp 70 and mouse anti-hsp 90 (StressGen, Victoria, BC, Canada), rabbit anti-GRP78/BiP (Santa Cruz Biotechnology, Santa Cruz, CA), horseradish peroxidase-conjugated rabbit anti-mouse IgG1 (Cappel, Durham, NC), horseradish peroxidase-conjugated sheep anti-mouse and horseradish peroxidase-conjugated donkey anti-rabbit antibodies (Amersham, Arlington Heights, IL). LysoTracker lysosomal marker was from Molecular Probes (Eugene, OR) and Cy3-conjugated anti-mouse and anti-goat antibodies were from Sigma Chemical. Monodansylcadaverine, epoxomicin, lactacystin, and other chemicals used in this study were purchased from Sigma Chemical.

Cell Lysate and Detergent-Insoluble Fractions

Exponentially growing MCF-7 cells were washed twice in ice-cold PBS and lysed on ice with TNESV buffer with added Complete protease inhibitor cocktail tablets (Roche Diagnostics, Penzberg, Germany). After centrifuging samples at 14,000 × *g* for 20 min at 4°C, the supernatant fraction was transferred to fresh tubes, and the NP40 detergent-insoluble fraction was resuspended in TNESV lysis buffer with protease inhibitors by brief sonication (10 s at 50 W on ice). Protein concentrations were determined spectrophotometrically by the microtiter plate bicinchoninic acid method using BSA as the standard (41) and samples were diluted with lysis buffer and reducing SDS loading buffer [100 mM DTT, 50 mM Tris-HCl (pH 6.8), 2% (w/v) SDS, 10% (v/v) glycerol, 0.01% (w/v) bromophenol blue tracking dye, final concentrations; Ref. 42] to the same protein content prior to running gels.

Immunoblotting Analysis

After fractionating samples by 10% SDS-PAGE, proteins were electrotransferred to Protran nitrocellulose membranes (Schleicher & Schuell, Keene, NH). Membranes used for anti-ubiquitin immunoblotting were autoclaved in deionized water for 20 min to denature bound ubiquitinated proteins, which exposes latent epitopes and increases the detection sensitivity (43). After blocking the membranes with 5% fat-free dry milk in 10 mM Tris (pH 7.5), 50 mM NaCl, 2.5 mM EDTA buffer, various antigens were immunodetected with appropriate primary antibodies followed by horseradish peroxidase-linked secondary antibodies. Visualization was by chemiluminescence (44) using a luminol-based commercial kit (Pierce Chemical Co., Rockford, IL), and exposed X-OMAT AR films (Kodak, Rochester, NY) were developed and scanned (Microtek Scanmaker III). The images were captured and processed with a Macintosh G4 computer using Adobe Photoshop 5.0 software and quantified using NIH Image 1.59 analysis software.

Analysis of Fluorescent Organelle Markers and Immunofluorescence

MCF-7 cells transfected with vectors expressing Living Colors organelle markers fused to enhanced yellow fluorescent protein 24 h previously were treated with 50 nM geldanamycin plus 10 nM bortezomib for 24 h to induce a vacuolated phenotype, and cells were examined directly for colocalization of organelle marker fluorescence with the drug-induced vacuoles. Other cells grown in glass chamber slides (Daigger & Co., Vernon Hills, IL) were treated with geldanamycin, bortezomib, or drug combination for 24 h, washed twice in PBS, and exposed to Karnovsky's fixative (Electron Microscopy Sciences, Fort Washington, PA) for 10 min. The cells were washed twice more in PBS and permeabilized with 0.2% Triton X-100 in PBS for 5 min. After washing cells in PBS thrice, nonspecific antibody binding was blocked by incubating with 5% BSA in PBS for 2 h at room temperature, and cells were washed again in PBS and exposed to the primary anti-ubiquitin or anti-hsp 70 (1:500 dilution) in a solution of 1% BSA in PBS for 2 h. Following three washes in PBS, cells were incubated with secondary Cy3-conjugated antibodies for 1 h in the dark. After three additional PBS washes, the fluorescence output was stabilized with two drops of SlowFade Light anti-fade mounting medium containing 4′,6-diamidino-2-phenylindole (Molecular Probes) to visualize nuclei, and the cells were examined with an IX50-FLA Olympus (Melville, NY) fluorescence microscope equipped with appropriate filters. Images were captured and processed on a Macintosh G4 computer using Adobe Photoshop software. In preliminary experiments, fixing cells with either cold acetone or methanol failed to preserve the drug-induced vacuolated morphology (data not shown).

LysoTracker and Monodansylcadaverine Fluorescence

To determine whether the geldanamycin plus bortezomib-induced vacuoles might be modified lysosomes or autophagosomes, we treated cells with 10 nM bortezomib and 50 nM geldanamycin for 18 h. The drug-containing medium was aspirated and replaced with fresh medium containing either LysoTracker lysosomal marker or the autophagosome probe, monodansylcadaverine, and both control and drug-treated cells were examined for colocalization of the chemical probes within the vacuoles by fluorescence microscopy.

Heat Shock

MCF-7 cells grown to subconfluency in 10 cm plates were placed in a humidified CO_2 incubator equilibrated and kept at 43°C for various times with and without bortezomib and geldanamycin.

Statistical Analysis

Where appropriate, data were analyzed by the two-sample, two-sided Student's *t* test (45), and differences between mean values at $P < 0.05$ were considered to be significant.

Results

Inhibition of Proteasome Activity in Cells by Bortezomib

We first determined a concentration and exposure time for bortezomib that would effectively inhibit proteasome activity in intact MCF-7 tumor cells. Exposing cells to a range of concentrations of bortezomib for as little as 1 h potently inhibited proteasome activity, yielding a calculated IC_{50} of 10 nM. At 25 nM, bortezomib inhibited proteasome activity greater than 90% within 1 h (Fig. 1A), and higher concentrations (up to 1 μM) did not appreciably further diminish proteasome activity (data not shown). Treatment with bortezomib for as long as 24 h similarly did not increase the magnitude of proteasome inhibition from that measured after 1 h (data not shown). Because bortezomib is a reversible proteasome inhibitor, we gauged its duration of action by exposing cells to 25 nM bortezomib for 2 h, removing the drug-containing medium and reincubating cells with fresh medium for various chase times. Bortezomib-inhibited proteasome activity returned slowly to its normal level by ~16 h (Fig. 1B). Because proteasome activity recovered when the bortezomib was removed, in subsequent experiments, we exposed cells continuously to the drug to maintain constant proteasome inhibition. While there were no overt signs of bortezomib cytotoxicity in cells exposed to 25 nM for as long as 24 h, by 48 h of bortezomib exposure, a few cells were rounded up, and eventually by 3 days, a large proportion of cells were nonadherent. Treating cells with the proteasome inhibitors epoxomicin and lactacystin also diminished proteasome activity, validating the assay for proteasome inhibition (data not shown). When as much as 2 μM geldanamycin was incubated with cells for 24 h or when geldanamycin was added directly to control cell lysates, it neither inhibited proteasome activity nor interfered with the recovery of proteasome activity following a short exposure to bortezomib (data not shown).

Bortezomib Enhances Geldanamycin Cytotoxicity to MCF-7 Cells

We next inquired whether the geldanamycin plus bortezomib combination would be more cytotoxic than either drug alone. Preliminary experiments revealed that both drugs inhibited MCF-7 cell proliferation at low nanomolar concentrations within 1 day, but neither drug was outright cytocidal within 3 days. We therefore selected several concentrations of bortezomib (2, 5 and 10 nM) and cotreated cells continuously with bortezomib and a range of geldanamycin concentrations from 2 to 100 nM for 3 days (Fig. 2A). Bortezomib at 2 nM had no influence on the antiproliferative activity of geldanamycin, 5 nM bortezomib with geldanamycin was slightly more effective than geldanamycin alone, but 10 nM bortezomib (~IC_{50} dose for proteasome inhibition) greatly enhanced the antiproliferative activity of geldanamycin and shifted the geldanamycin concentration *versus* survival curve nearly 1.5 logs (Fig. 2A). Bortezomib itself caused a concentration-dependent inhibition of cell proliferation, diminishing growth by nearly 90% within 3 days when used at 10 nM (Fig. 2B).

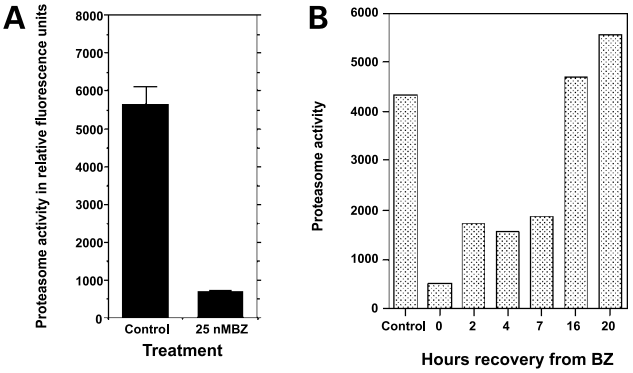

Figure 1. Proteasome activity after bortezomib treatment. Cells were treated with bortezomib, and proteasome activity was measured in 10 μl aliquots of lysates using a synthetic fluorogenic peptide substrate. **A,** cells were treated with 25 nM bortezomib for 1 h; control cells were exposed to an equivalent DMSO. *Columns,* mean proteasome activity in arbitrary relative fluorescence units ($n = 6$); *bars,* SD. Proteasome activity after bortezomib was significantly decreased as determined by Student's t test at $P < 0.001$. **B,** cells were exposed to 25 nM bortezomib for 2 h and then washed and incubated in fresh medium for the indicated times before cell lysis and assay of proteasome activity. *Bars,* mean of duplicate values; therefore, the SD was not displayed.

While neither geldanamycin nor bortezomib alone, even at high concentrations, maximally inhibited cell proliferation by more than 90%, the combination of the two drugs inhibited tumor cell proliferation nearly 99.9% (Fig. 2A).

We next exposed cells continuously to a range of geldanamycin concentrations without or with 10 nM bortezomib for 4 days. In this experiment, as before, geldanamycin was predominantly cytostatic, with little difference in its ability to inhibit proliferation between 100 nM and 1 μM. When geldanamycin was combined with 10 nM bortezomib, the drug combination became cytocidal, with essentially no surviving cells after 4 days of exposure (Fig. 2C). This observation was validated using trypan blue nuclear staining, which indicated that essentially all cells were dead (data not shown).

Because geldanamycin and bortezomib might not be administered to patients simultaneously, we investigated whether a sequential addition of geldanamycin and bortezomib would still be capable of enhancing antiproliferative activity. Exposing cells sequentially to geldanamycin and bortezomib, with either drug added first for 24 h, was only slightly more effective in inhibiting cell proliferation than either drug used alone (Fig. 2, D and E). Finally, we performed an experiment where cells were exposed to concentrations of both drugs fixed at a 1:1 ratio, beginning at 1 nM and escalating up to 100 nM. Note that 100 nM bortezomib alone was not much more effective than 10 nM bortezomib. However, again, the geldanamycin plus bortezomib combination was superior to either drug alone (Fig. 2F). Taken together, these data reveal that bortezomib, at a low 10 nM concentration just sufficient to inhibit the proteasome by ~50%, enhanced the antiproliferative activity of geldanamycin against MCF-7 cells by more than 10-fold.

Bortezomib plus 17-AAG Is Preferentially Cytotoxic to Transformed Cells

We next compared the relative cytotoxicity of 17-AAG, bortezomib, and the combination of bortezomib plus 17-AAG toward nontransformed and transformed NIH 3T3 fibroblasts stably transfected with and selected for expression of genes encoding HPV16-E6 or both HPV16-E6 and HPV16-E7 proteins. The expression levels of E6 and E7 proteins in these stably transfected cells have been measured previously (38, 46). Cells expressing HPV16-E6 protein and, to a greater extent, both E6 and E7 proteins (HPV18-E6/E7) clearly display a malignant phenotype characterized by lack of contact inhibition, proliferation in soft agar, and rapid growth in nude mice (47, 48). Thus, these particular transformed cell lines provide a reasonable model system that mimics the behavior of normal (albeit immortalized), malignant (E6 alone), and aggressively malignant (E6 and E7) tumor cells, respectively.

Bortezomib alone at 25 nM did not affect the clonogenicity of the LXSN vector control cells, the HPV16-E6 transformed cells, or the HPV18-E6/E7 transformed cells. Similarly, 17-AAG alone was not cytotoxic to LXSN cells at any concentration up to and including 50 nM, the highest concentration tested, while HPV16-E6 cells and, to a slightly greater extent, HPV18-E6/E7 cells were modestly sensitive to 17-AAG (Fig. 3, A–C). In contrast, when the transformed HPV16-E6 cells and the more aggressive HPV18-E6/E7 cells were exposed to the combination of bortezomib plus 17-AAG, there was a statistically

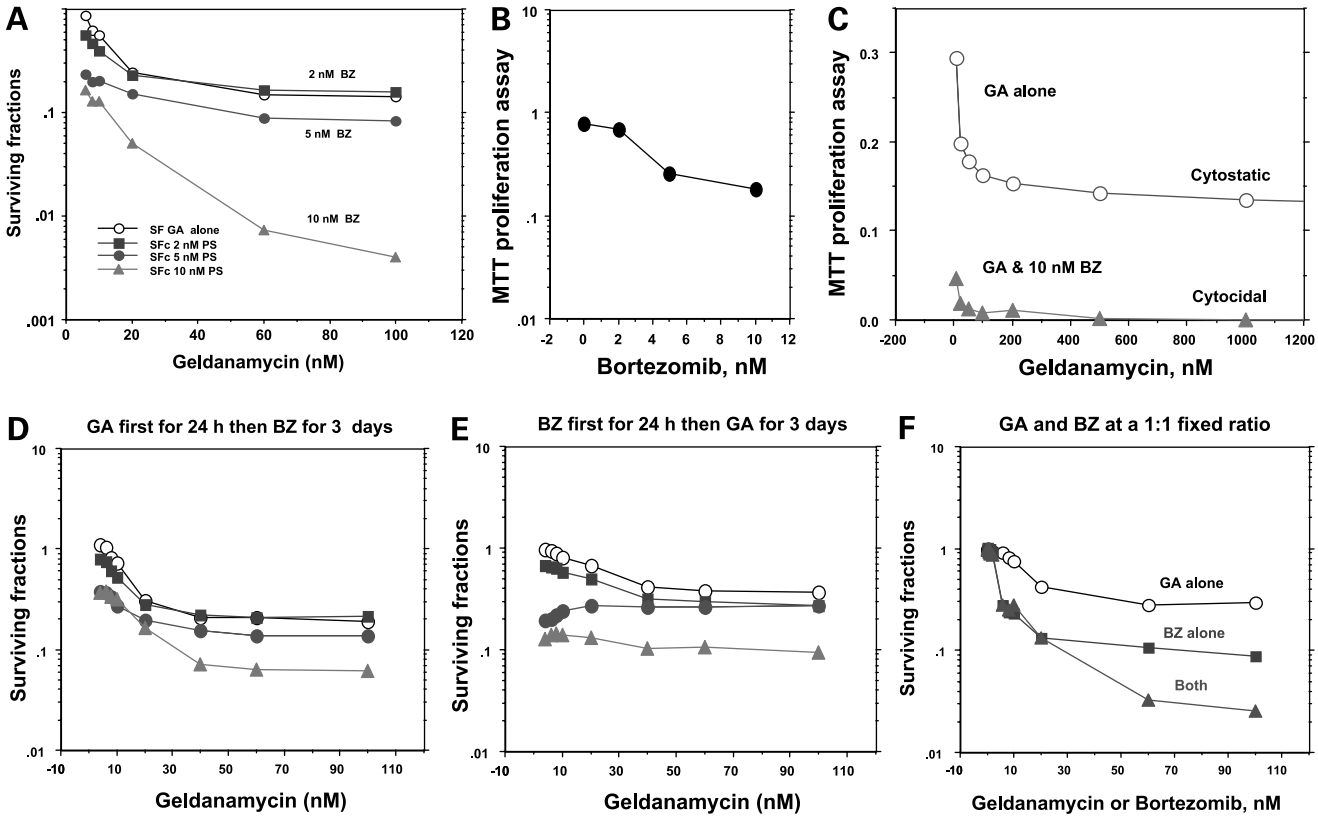

Figure 2. Geldanamycin and bortezomib show enhanced antiproliferative activity in combination and convert cytostasis to a cytocidal outcome. MCF-7 cells were seeded into 96-well plates; 24 h later, they were treated with geldanamycin and bortezomib (six wells/concentration) as indicated in **A–C**. Antitumor activity was assessed 3 or 4 days later by the 3-(4,5-dimethylthiazol-2-yl)-2,5-diphenyltetrazolium bromide spectrophotometric assay. **A,** surviving fractions of cells are shown after 3 days exposure to a range of concentrations of geldanamycin alone (*open circles*) or with 2 nM (*shaded squares*), 5 nM (*shaded circles*), or 10 nM (*triangles*) bortezomib. **B,** antiproliferative affect of bortezomib alone after 3 days of exposure. **C,** cells were exposed to a range of geldanamycin concentrations without (*open circles*) and with 10 nM (*triangles*) bortezomib for 4 days. Note that geldanamycin alone was cytostatic, and concentrations above 100 nM did not yield any additional antiproliferative activity. Exposing cells to bortezomib alone for 4 days was about as effective as 3 days, but when geldanamycin was combined with bortezomib, the number of surviving cells decreased dramatically to essentially zero, indicating that the drug combination was cytocidal (**D**). In this experiment, cells were exposed to a range of concentrations of geldanamycin for 24 h; then, medium (*open circles*) or bortezomib at 2 nM (*shaded squares*), 5 nM (*shaded circles*), and 10 nM (*triangles*) was added for an additional 3 days. **E,** medium only (*open circles*) or bortezomib at 2 nM (*shaded squares*), 5 nM (*shaded circles*), and 10 nM (*triangles*) was added to cells first for 24 h; then, geldanamycin at various concentrations was added for an additional 3 days. **F,** geldanamycin and bortezomib were combined at a fixed ratio of 1:1, serially diluted, and added to cells for 3 days. Geldanamycin alone (*open circles*), bortezomib alone (*shaded squares*), or both drugs (*shaded triangles*) were at the concentrations indicated on the *abscissa*. *Points,* mean of six wells; SD typically were less than 5% of mean values.

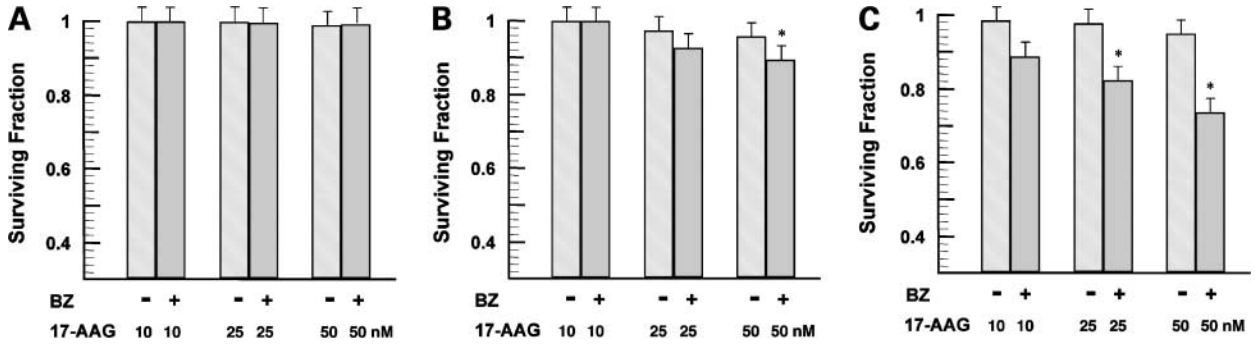

Figure 3. Bortezomib and 17-AAG are preferentially cytotoxic to HPV E6 and E7 transformed immortalized cells. Clonogenic cell survival results showing the effects of a 24 h exposure to 17-AAG alone (10, 25, or 50 nM) and 17-AAG combined with 25 nM bortezomib to NIH 3T3 cells stably transfected with either empty vector (**A**) or viral expression vectors encoding *HPV16-E6* (**B**) or *HPV16-E6* and *HPV16-E7* (**C**) genes. Ten days after drug exposures, colonies were stained and scored and the normalized surviving fractions were plotted against drug concentrations. *Columns,* mean; *bars,* 1 SD about the arithmetic mean. *, $P < 0.05$, statistically significant differences between identically treated samples within the control, E6-expressing, and E6/E7-expressing cells (Student's paired *t* test; $n = 6$).

significant increase in cell killing compared with the affects of either drug alone (Fig. 3, B and C). There was no cytotoxicity to the LXSN ''normal'' parental fibroblasts at any of the drug combinations used in this series of experiments. In this model system, bortezomib combined with 17-AAG was clearly more potent against the viral oncogene-transformed cells with malignant characteristics when compared with ''normal'' immortalized fibroblasts.

Treatment with Geldanamycin and Bortezomib Enhances the Accumulation of Detergent-Insoluble Ubiquitinated Proteins

Preliminary experiments revealed that in MCF-7 cells exposed to various concentrations of bortezomib for 24 h, ubiquitinated proteins were stabilized in the clarified lysate and detergent-insoluble pellet fractions of lysed cells measured by anti-ubiquitin immunoblotting (Fig. 4A). Following treatment with as little as 10 nM bortezomib ($\sim IC_{50}$ for proteasome inhibition; in this report), a large quantity of ubiquitinated proteins was found in the lysate fraction, while only a slight increase in protein ubiquitination was found in the pellet fraction (Fig. 4A, *top and bottom panels*). The extent of protein ubiquitination was substantially increased in the pellet fraction of cells exposed to 25 nM bortezomib ($\sim IC_{90}$), but higher concentrations of bortezomib did not further augmented the extent of protein ubiquitination in either fraction (Fig. 4A). These data suggest that ubiquitinated proteins first accumulated in the cytosol and became aggregated and relocated into the detergent-insoluble fraction of cells when proteasomes are inhibited beyond a threshold level. In contrast, while treating cells with as much as 1 μM geldanamycin did not increase protein ubiquitination in cell lysates, this high concentration of geldanamycin slightly elevated the level of protein ubiquitination in the insoluble fraction, provided the film was exposed for a long time (Fig. 4B, *lower panel*).

We next determined whether geldanamycin might enhance protein ubiquitination in the presence of 10 nM bortezomib. Although geldanamycin plus bortezomib did not increase protein ubiquitination in the lysate fraction beyond the level that was stabilized by bortezomib, geldanamycin greatly enhanced protein ubiquitination in the detergent-insoluble fraction of cells cotreated with 10 nM bortezomib (Fig. 4B). Note that in comparing the amounts of protein ubiquitination in the lysate and pellet fractions, twice as much lysate protein as pellet protein was loaded onto gels. The massive increase in ubiquitinated proteins in the detergent-insoluble fraction following geldanamycin plus bortezomib cotreatment suggests that those proteins were aggregated. It is also likely that the increase in ubiquitinated proteins in the insoluble fraction of cells treated with geldanamycin plus bortezomib were hsp 90 client proteins.

Other hsp 90 Inhibitors Can Substitute for Geldanamycin

To verify the hsp 90 dependency of the increased protein ubiquitination in geldanamycin plus bortezomib-treated cells, we conducted experiments with several other hsp 90 inhibitors: 17-AAG, radicicol, radicicol oxime, and WX514, an ansamycin known to specifically interact strongly with hsp 90 but only weakly with GRP94, the hsp 90 homologue in the ER (49). As shown in Fig. 5, A–C, each of these hsp 90-targeting agents dramatically enhanced protein ubiquitination in the detergent-insoluble pellet fraction of tumor cells cotreated with bortezomib. In the absence of bortezomib, none of the hsp 90-targeting drugs, even at very high concentrations, caused more than a slight increase in protein ubiquitination in the clarified lysate fraction of cells (data not shown). On the other hand, geldampicin, a benzoquinone ansamycin that does not interact with hsp 90 and does not down-regulate hsp 90 client proteins, did not increase protein ubiquitination when combined with bortezomib (Fig. 5D). These results reinforce our interpretation that a large proportion of the ubiquitinated proteins in cells treated with geldanamycin plus bortezomib were destabilized hsp 90 client proteins. Although not shown here, several other proteasome

inhibitors (epoxomicin, lactacystin, MG132, and ALLnL), when combined with 50 nM geldanamycin, also strongly promoted protein ubiquitination in the detergent-insoluble fraction of tumor cells, ruling out any spurious effects of bortezomib.

Geldanamycin and Bortezomib Induce the Cellular Stress Response

When cells are heated or exposed to certain noxious chemicals, they initiate a defensive heat shock response or stress response (50, 51). Under these conditions, the expression of numerous protein chaperones, including hsp 90 and hsp 70, is greatly increased (52). Both geldanamycin and proteasome inhibitors are known to induce a strong heat shock response in cells (53–56), and we wondered whether simultaneous geldanamycin plus bortezomib exposure might elicit an even more powerful heat shock response. When used alone, in both clarified lysate and detergent-insoluble fractions, hsp 90, hsp 70, and the ER-residing protein chaperone, GRP78/BiP, were increased as much as 10-fold by geldanamycin in a concentration-dependent fashion (Fig. 6). Similarly, bortezomib alone elevated all three of these stress proteins. Especially interesting was the appearance of appreciable quantities of hsp 90, hsp 70, and GRP78/BiP in the detergent-insoluble pellet fraction from cells treated with geldanamycin plus bortezomib (Fig. 6). Stress proteins have been found associated with large aggregates of misfolded proteins called aggresomes (57, 58), and it is probable that these three stress proteins in the detergent-insoluble fraction of geldanamycin and bortezomib-treated cells were similarly associated with aggregated and ubiquitinated proteins.

Sequential Exposure to Bortezomib and Geldanamycin Increases Ubiquitination

To determine whether it was necessary to simultaneously expose cells to geldanamycin plus bortezomib to enhance protein ubiquitination, we treated MCF-7 cells with bortezomib for 2 h and aspirated the drug, and after a wash with complete medium, either fresh medium or geldanamycin-containing medium was added, and the cells were incubated for 4, 16, and 24 h chase times. At 16 and 24 h post-bortezomib, protein ubiquitination was increased (Fig. 7A), although proteasome activity recovers from bortezomib exposure by ~16 h (Fig. 1B). The addition of

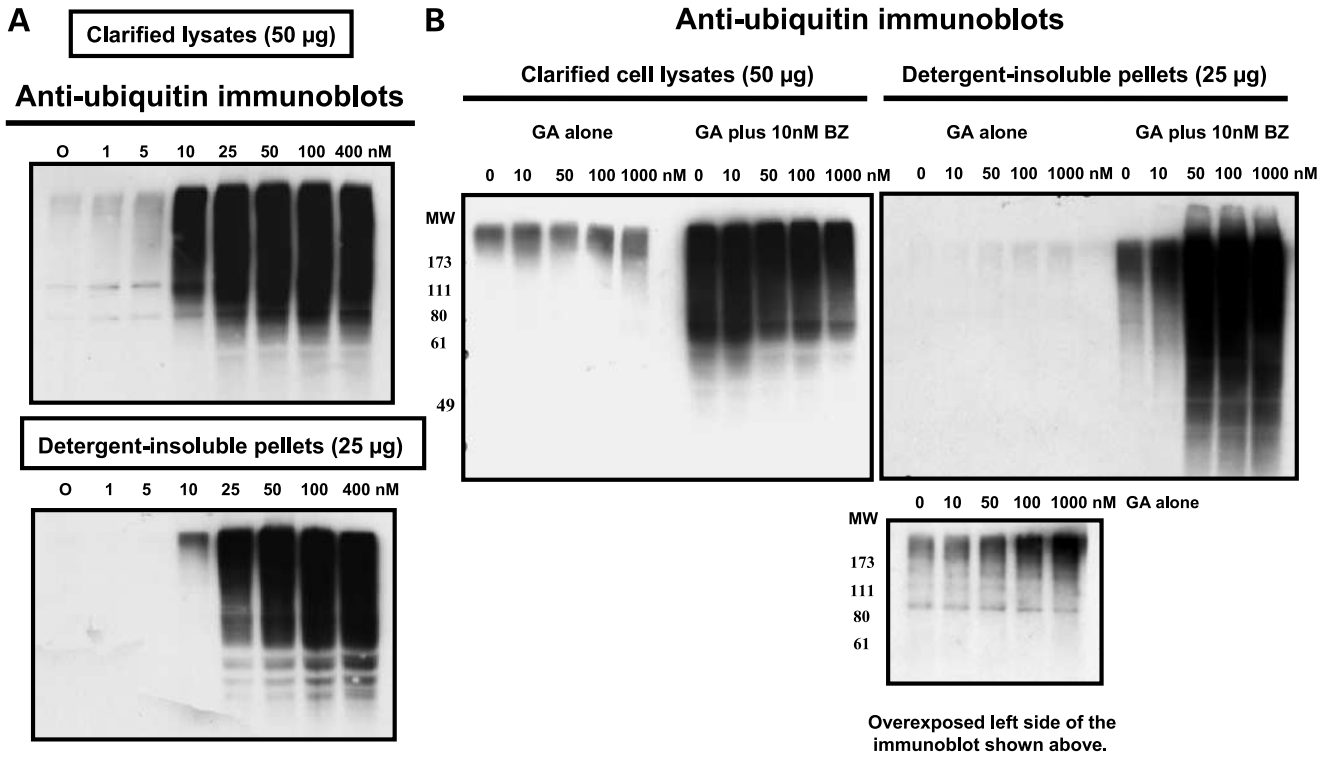

Figure 4. Geldanamycin and bortezomib enhance protein ubiquitination. MCF-7 tumor cells were treated with bortezomib alone, geldanamycin alone, or various combinations of the two drugs for 24 h before cell lysis. Lysates were separated into clarified lysate (soluble proteins) and detergent-insoluble pellet fractions; after protein assay, SDS-PAGE separation, and transfer, nitrocellulose membranes were autoclaved, blocked, and immunoblotted for ubiquitin. **A,** cells were exposed to a range of concentrations of bortezomib alone. Note that high molecular weight ubiquitinated proteins accumulated in both lysate and detergent-insoluble pellet fractions. **B,** cells were treated with a range of geldanamycin concentrations without or with 10 nM bortezomib, the lowest concentration of bortezomib that caused ubiquitinated proteins to accumulate. There was no increase in protein ubiquitination in lysates from cells treated with geldanamycin alone, while in the pellet fraction, geldanamycin slightly increased the low level of ubiquitination that could be visualized only after a long film exposure (*bottom panel*). Geldanamycin combined with bortezomib did not further increase protein ubiquitination in lysates, but geldanamycin and bortezomib greatly increased the level of ubiquitinated proteins that were redistributed to the pellet fraction. When the lanes showing protein ubiquitination in the detergent-insoluble fractions were measured by densitometry, geldanamycin plus bortezomib caused 3.9-fold more protein ubiquitination than the sum of the individual ubiquitination values caused by geldanamycin and bortezomib separately.

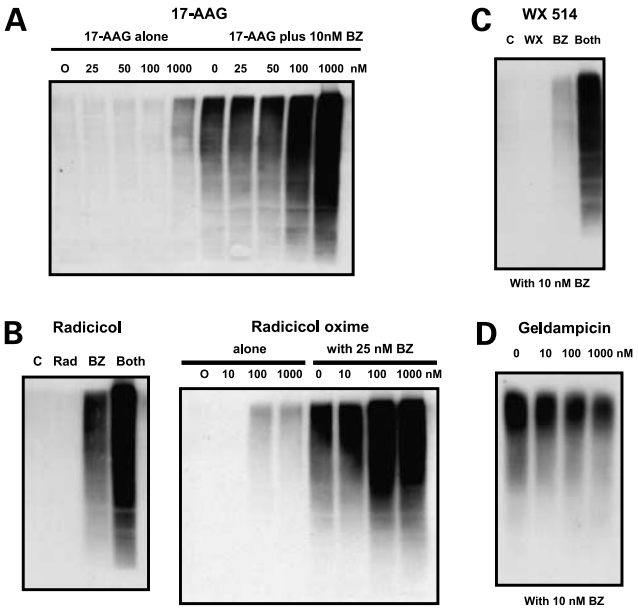

Figure 5. Other specific hsp 90 inhibitors enhance ubiquitination of insoluble aggregated proteins when combined with bortezomib. MCF-7 tumor cells were treated with various hsp 90 inhibitors, without or with 10 or 25 nM bortezomib, as indicated, and protein ubiquitination in the detergent-insoluble fraction was measured by anti-ubiquitin immunoblotting. **A,** cells were incubated with several concentrations of 17-AAG, the clinical analogue of geldanamycin. Note that 17-AAG alone, at the highest concentration, only slightly increased protein ubiquitination, but 17-AAG combined with bortezomib increased ubiquitination more than 10-fold. **B,** radicicol (100 nM) or radicicol oxime was combined with 25 nM bortezomib. **C,** WX514 at 3 μM was combined with 25 nM bortezomib. **D,** geldampicin, an ansamycin that does not bind to hsp 90 and cannot destabilize hsp 90 client proteins, was combined with 10 nM bortezomib. Note that geldampicin did not increase protein ubiquitination in the detergent-insoluble fraction beyond the quantity stabilized by bortezomib treatment.

geldanamycin during the chase more than doubled the quantity of ubiquitinated proteins measured at 16 and 24 h after bortezomib washout. These results indicate that the massive amount of ubiquitinated proteins in bortezomib plus geldanamycin sequentially treated cells must have overwhelmed the ability of proteasomes to clear them, even when bortezomib was removed and activity returned to normal.

Cycloheximide Blocks Geldanamycin plus Bortezomib-Stimulated Protein Ubiquitination

Geldanamycin prevents hsp 90-dependent maturation of many newly synthesized proteins (4, 59), and we wondered whether increased protein ubiquitination caused by geldanamycin plus bortezomib might represent selective ubiquitination of newly synthesized proteins. To explore this possibility, we pretreated cells with cycloheximide for 30 min prior to exposing them to geldanamycin, bortezomib, or drug combination. Protein ubiquitination caused by bortezomib alone, as well as ubiquitination enhanced by bortezomib plus geldanamycin, in both clarified and insoluble pellet fractions was completely blocked by cycloheximide (Fig. 7B). Interestingly, cycloheximide also diminished the low level of protein ubiquitination in control cell lysates. The induction of hsp 70 and hsp 90 caused by geldanamycin, bortezomib, or drug combination was also cycloheximide sensitive, verifying that protein synthesis had been inhibited (Fig. 7B, *bottom panels*). These data imply that newly synthesized proteins, especially hsp 90 client proteins, may be extraordinarily susceptible to ubiquitination perhaps because they were incompletely folded into their mature conformation. It is also possible that a large increase in protein ubiquitination would require supplemental synthesis of ubiquitin, which cycloheximide prevented.

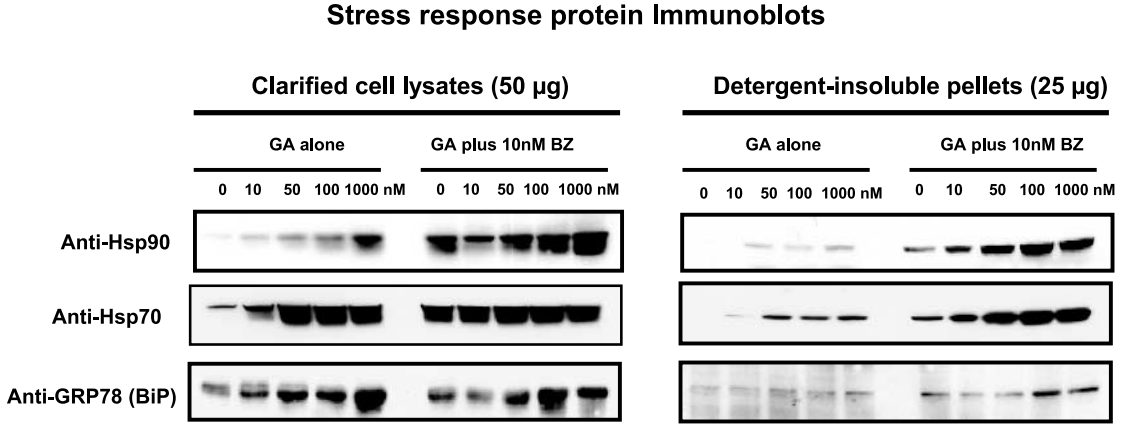

Figure 6. Geldanamycin and bortezomib enhance the cellular stress response and drive protein chaperones into the detergent-insoluble fraction. Cells were treated exactly as described in Fig. 2, and clarified lysate and detergent-insoluble pellet fractions were run on 10% SDS-PAGE, transferred to nitrocellulose, and probed for hsp 90, hsp 70, and GRP78/BiP. Both geldanamycin and bortezomib alone increased chaperone protein levels found in lysates, and geldanamycin combined with bortezomib caused a synergistic relocalization of substantial quantities of the three chaperone proteins to the detergent-insoluble fraction. Comparing the profile of the stress proteins in the pellet fraction in this figure with the profile of protein ubiquitination in Fig. 2 shows that stress protein induction and relocalization coincided with the accumulation of aggregated and insoluble ubiquitinated proteins. Densitometry of each of the hsp 70 and hsp 90 bands in the detergent-insoluble fraction of cells treated with geldanamycin, bortezomib, or both drugs was conducted, and a 3.2-fold higher level of hsp 90 and a 1.6-fold higher level of hsp 70 resulted from the geldanamycin plus bortezomib combination treatment than the sum of the hsp 90 and hsp 70 levels induced by bortezomib and geldanamycin separately.

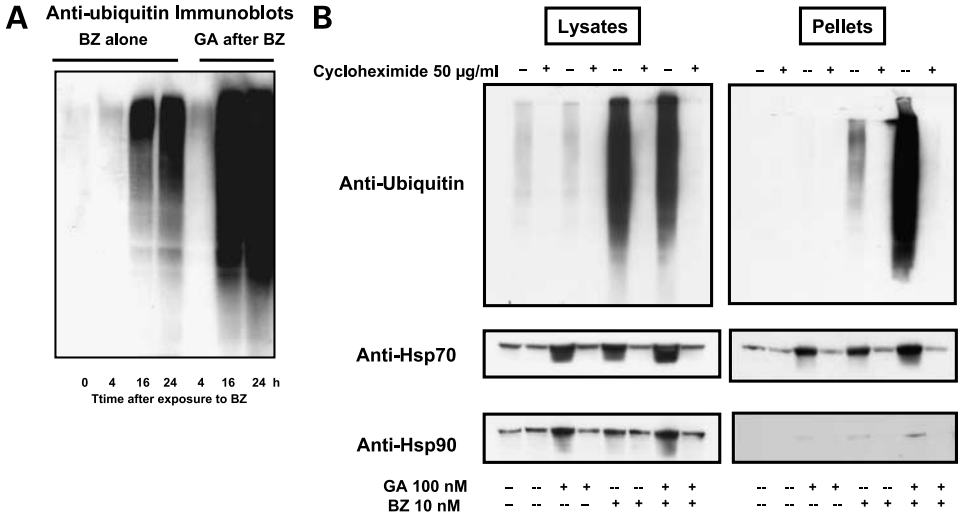

Figure 7. Geldanamycin and bortezomib increase ubiquitination when used sequentially, and geldanamycin plus bortezomib-enhanced protein ubiquitination is blocked by cycloheximide. MCF-7 cells were first exposed to 25 nM bortezomib for 2 h, the drug was aspirated, and the cells were washed with medium and incubated with fresh medium for 4, 16, and 24 h without and with 500 nM geldanamycin. Cell lysates were prepared, proteins were separated by 10% SDS-PAGE, and the nitrocellulose membrane was immunoblotted for ubiquitin. **A,** although there was no increase in protein ubiquitination after 4 h chase, ubiquitination was greatly increased 16 and 24 h after removal of bortezomib. This indicates that cells had acquired sufficient drug to inhibit the proteasome for an extended time, thus permitting ubiquitinated proteins to accumulate even after the drug had been removed from the medium. Inclusion of geldanamycin during the chase time, after bortezomib was removed, further increased protein ubiquitination over the level caused by bortezomib alone. **B,** cells were treated with 10 nM bortezomib, 100 nM geldanamycin, or both drugs without and with 50 μg/ml cycloheximide to prevent protein synthesis. In all instances, in both lysate and pellet fractions, cycloheximide completely blocked drug-stimulated protein ubiquitination and prevented the induction of hsp 90 and hsp 70.

Geldanamycin plus Bortezomib Induces Prominent Perinuclear Vacuoles

While conducting these experiments, we observed that a high proportion of MCF-7 cells exposed to geldanamycin plus bortezomib became nearly filled with cytoplasmic vacuoles (Fig. 8, *top panels*). This conspicuous morphological response to these drugs did not occur in cells treated with as much as 1 μM geldanamycin alone or with 10 nM bortezomib alone for 24 h, although bortezomib at 25 nM or higher concentrations caused a slight amount of vacuolization in a small percentage of cells. By 48 h exposure to geldanamycin plus bortezomib, more than 50% of cells were extensively vacuolated. Monitoring the time course of bortezomib plus geldanamycin-induced vacuolization by microscopy revealed that the vacuoles were initially few, small, and predominantly perinuclear localized within the first 12–18 h. The numerous small vacuoles later increased in number and coalesced into larger vacuoles, which eventually occupied the entire cytoplasmic space. Moreover, if geldanamycin and bortezomib were removed after 24 h and cells were incubated with fresh medium, the drug-induced vacuoles regressed and eventually disappeared. Close examination by high-power phase contrast microscopy suggested that the vacuoles were membrane bound. This possibility was strengthened by the observation that when 1% NP40 detergent-containing lysis buffer or the organic solvent fixatives methanol and acetone were gently washed onto cells, the vacuoles disappeared within a few seconds, most likely because their enveloping membranes dissolved (data not shown).

To characterize the origin of the vacuoles, we transfected MCF-7 cells with plasmids expressing Living Colors yellow fluorescent protein-fusion organelle markers for Golgi, ER, and plasma membrane. After 24 h, transfected cells were treated with 50 nM geldanamycin and 25 nM bortezomib for an additional 24 h. Fluorescent microscopy indicated that of the three organelle marker probes, only the ER marker-derived yellow fluorescent protein localized with the drug-induced vacuoles. In control cells, the ER marker yellow fluorescent protein was diffuse, cytoplasmic, and reticular, while the ER marker fluorescence in geldanamycin plus bortezomib-treated cells was observed predominantly within the vacuoles or possibly on the vacuole surface (Fig. 8, *lower four panels*). Interestingly, heat shocking cells at 42°C for 4 h in the presence of bortezomib, but not heat shock alone, also induced cells to form identical-appearing vacuoles (Fig. 9, *bottom two panels*), suggesting that any stressor promoting the accumulation of misfolded, ubiquitinated proteins within the ER may have the potential to induce cell vacuolization. Geldanamycin plus bortezomib also induced the vacuolated phenotype in PC-3 prostate carcinoma cells, RCC-C2 renal carcinoma cells, and COS-7 monkey kidney cells, which were especially responsive to geldanamycin plus bortezomib, indicating that MCF-7 cells were not a special case (data not shown). A similar cellular vacuolization phenomenon in response to the proteasome inhibitor, PSI, has been reported previously (60).

To confirm a requirement for proteasome inhibition to induce cells to generate the vacuole phenotype, we replaced

bortezomib with lactacystin, epoxomicin, or ALLnL. These proteasome inhibitors, when combined with geldanamycin, were all capable of causing cells to become vacuolated (data not shown). To verify the hsp 90 dependence of the vacuolization, we substituted 17-AAG, radicicol, or radicicol oxime for geldanamycin and observed that each of these hsp 90 inhibitors induced a perfusion of vacuoles in MCF-7 cells but only when they were coincubated with bortezomib (Fig. 9, *top eight panels*). Note that 25 nM bortezomib alone induced only a few vacuoles in an occasional cell. These data confirm previous results, which indicated that vacuolization was dependent on inhibition of both hsp 90 and proteasomes.

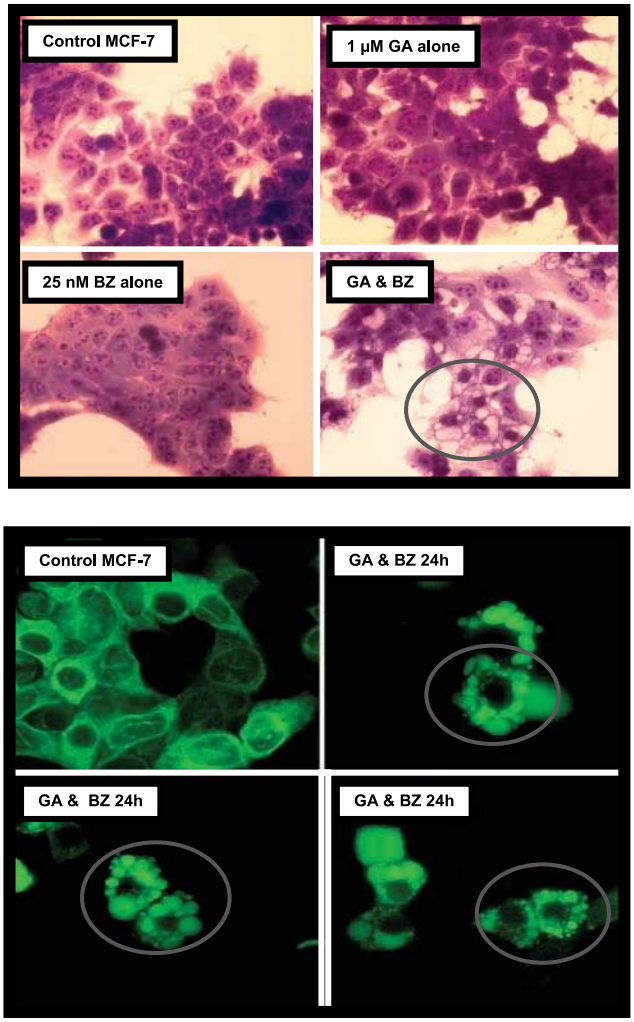

Figure 8. Vacuolization in MCF-7 cells after geldanamycin and bortezomib. Tumor cells were treated with the indicated concentrations of geldanamycin or bortezomib alone or with the combination of both drugs for 24 h. **A,** cells were washed in PBS, fixed in formalin, and stained with Diff-Quick (*top four panels*). Note that vacuoles are present only in the cells treated simultaneously with both drugs. **B,** cells were transfected with a vector expressing Living Colors fluorescent ER marker yellow fluorescent protein-fusion protein using FuGene, treated with 25 nM bortezomib or 50 nM geldanamycin alone or the combination of drugs for 24 h, and photographed using a fluorescent microscope at ×200 magnification (*bottom four panels*). Fluorescence from the ER marker was diffuse and cytoplasmic in control cells, while in geldanamycin and bortezomib-treated cells, the ER marker strongly colocalized with the vacuoles.

Cycloheximide Prevents Geldanamycin plus Bortezomib-Induced Cell Vacuolization

Because we observed previously that cycloheximide blocked geldanamycin plus bortezomib-induced protein ubiquitination, we asked whether cycloheximide might also prevent geldanamycin plus bortezomib-caused vacuolization. In tumor cells cotreated with geldanamycin, bortezomib, and cycloheximide, the conspicuous vacuoles observed by phase contrast in geldanamycin plus bortezomib-treated cells were completely absent (Fig. 10, *top row*). The ability of cycloheximide to prevent vacuolization was verified in cells transfected with the Living Colors yellow fluorescent protein-fusion ER marker plasmid. Following geldanamycin plus bortezomib and cycloheximide cotreatments, ER marker fluorescence was essentially identical to that observed in control ER marker-transfected cells, while in cells not exposed to cycloheximide, the geldanamycin plus bortezomib-induced, ER-derived fluorescent vacuoles were in abundance (Fig. 10, *bottom row*). These data support the concept that newly synthesized, ER-localized hsp 90 client proteins destabilized by geldanamycin were unable to undergo retrograde translocation from the ER through exit translocons into the cytosol when proteasomes were inactivated by bortezomib. These observations are consistent with our proposal that the profound ER stress induced by geldanamycin plus bortezomib exposure provokes cells to defensively form ER-derived vacuoles in an attempt to relieve a backup of misfolded proteins stalled within the ER lumen.

The Geldanamycin and Bortezomib-Induced Vacuoles Do Not Contain Ubiquitin or hsp 70

Because geldanamycin plus bortezomib-induced vacuoles were closely associated with enhanced protein ubiquitination, we suspected the vacuoles might contain engulfed ubiquitinated proteins. To investigate this possibility, we treated cells with both drugs and attempted to visualize ubiquitinated proteins inside the vacuoles by anti-ubiquitin immunofluorescence. Although many vacuolated cells were easily observed by phase contrast microscopy, anti-ubiquitin fluorescence was diffuse, cytoplasmic, and clearly was not colocalize with vacuoles. This is most easily seen in the layered phase contrast and anti-ubiquitin fluorescence photograph, where the red anti-ubiquitin signal is conspicuously excluded from the vacuoles (Fig. 11, *row A*). We then attempted to find another abundant cytoplasmic protein, hsp 70, inside the vacuoles. Hsp 70 is known to facilitate ER-associated degradation of the cystic fibrosis transmembrane conductance regulator (61); therefore, it might participate in the formation of ER-derived vacuoles. We found instead that anti-hsp 70 immunofluorescence was restricted to the cytoplasm and was completely excluded from the vacuoles (Fig. 11, *row B*). In fact, a few larger vacuoles can be seen as dark spots against red anti-hsp 70 immunofluorescence, and the vacuoles appear as light spots in the phase contrast

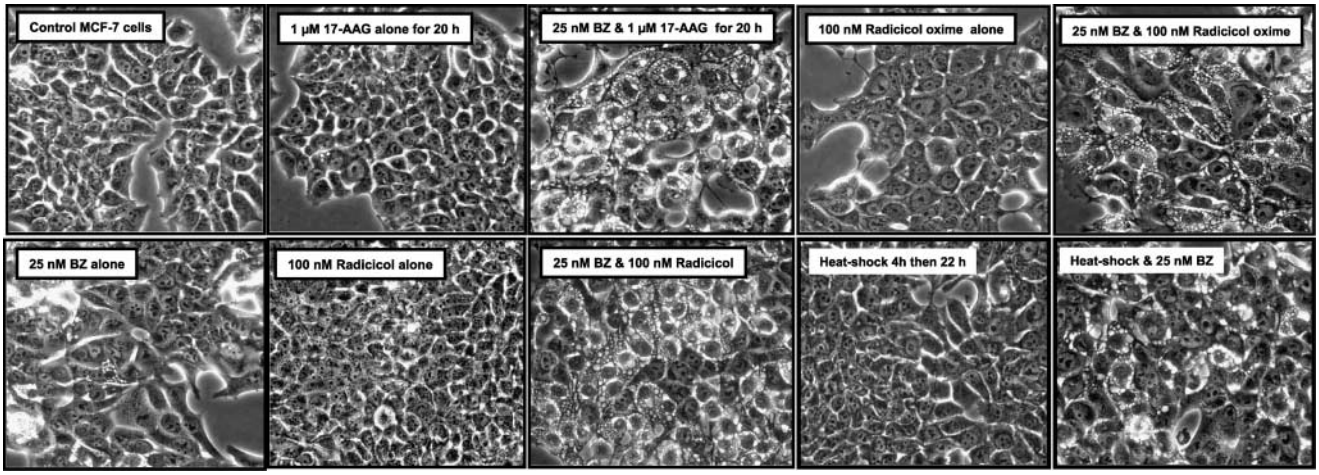

Figure 9. Other hsp 90-targeting drugs and heat shock, when combined with bortezomib, cause cell vacuolization. MCF-7 tumor cells were treated with 17-AAG, radicicol, radicicol oxime, or heat shock in place of geldanamycin, without and with 25 nM bortezomib for 18 – 24 h, and examined by phase contrast microscopy. Neither the hsp 90-targeting drugs at high concentrations nor heat shock alone caused cells to form vacuoles, while bortezomib alone induced only a few vacuoles in a few cells. In contrast, when combined with bortezomib, all of the hsp 90-targeting drugs as well as heat shock caused extensive cell vacuolization.

and anti-hsp 70 immunofluorescence layered composite (Fig. 11, *row B*). Based on these observations, it is unlikely that the vacuoles contain other engulfed cytoplasmic proteins.

Finally, we investigated whether the geldanamycin plus bortezomib-induced vacuoles might be either modified lysosomes or autophagosomes recruited in response to the massive accumulation of undegraded ubiquitinated proteins. We used the LysoTracker fluorescent probe to identify lysosomes (Fig. 11, *row C*) and monodansylcadaverine fluorescence to identify autophagosomes (Fig. 11, *row D*). Although these two fluorescent probes successfully visualized their intended target organelles, neither probe associated with the drug-induced vacuoles, ruling out the possibility that the drug-induced vacuoles filling the cells were lysosomes or autophagosomes.

Discussion

Geldanamycin and bortezomib are especially fascinating because each drug has a specific molecular target, yet by interacting with their targets, these drugs interfere with the function of myriad critical regulators of cell proliferation, angiogenesis, adhesion, and survival (7, 62–64). The binding of geldanamycin to hsp 90 destabilizes its numerous client proteins, which become ubiquitinated and are then degraded by proteasomes. We speculated that if, at the same time, proteasomes were to be inhibited by bortezomib, the torrent of geldanamycin-destabilized, ubiquitinated proteins would aggregate and accumulate to cytotoxic levels. Recently, Mitsiades *et al.* (25) provided encouraging support for this concept by showing that an analogue of geldanamycin enhanced the antiproliferative activity of bortezomib.

In the absence of proteasome inhibition, in geldanamycin-treated cells, ubiquitinated hsp 90 client proteins are rapidly degraded (5, 6, 8, 65, 66), and consequently, we were able to detect only a minuscule increase in protein ubiquitination following geldanamycin alone. Complete inhibition of proteasome activity with a high concentration of bortezomib stabilizes essentially all ubiquitinated proteins, making any geldanamycin-dependent increase in protein ubiquitination impossible to detect. By titrating the concentration of bortezomib to only partially inhibit proteasome activity, we were able to demonstrate an enormous geldanamycin-dependent increase in protein ubiquitination. It is noteworthy that the majority of geldanamycin-enhanced, bortezomib-stabilized ubiquitinated proteins accumulated in the detergent-insoluble fraction of cell lysates, supporting our hypothesis that they would become misfolded and aggregated. There is considerable evidence that aggregated ubiquitin protein conjugates are pathogenic in a broad collection of human degenerative diseases (64).

The antiproliferative activity of geldanamycin plus bortezomib against MCF-7 cells, at clinically achievable concentrations, was much greater than the activity of either geldanamycin or bortezomib alone. Moreover, simultaneous exposure to geldanamycin plus bortezomib was considerably more effective than sequential exposure to the two drugs, emphasizing the importance of geldanamycin and bortezomib interdependent action to the antitumor effects of the drug combination. While geldanamycin and bortezomib, as single agents, were cytostatic against MCF-7 cells, the geldanamycin plus bortezomib drug combination was cytocidal. This is an important distinction because the small fraction of tumor cells that survive chemotherapy often become drug resistant.

While our results fall short of establishing an unequivocal cause-and-effect relationship between the massive

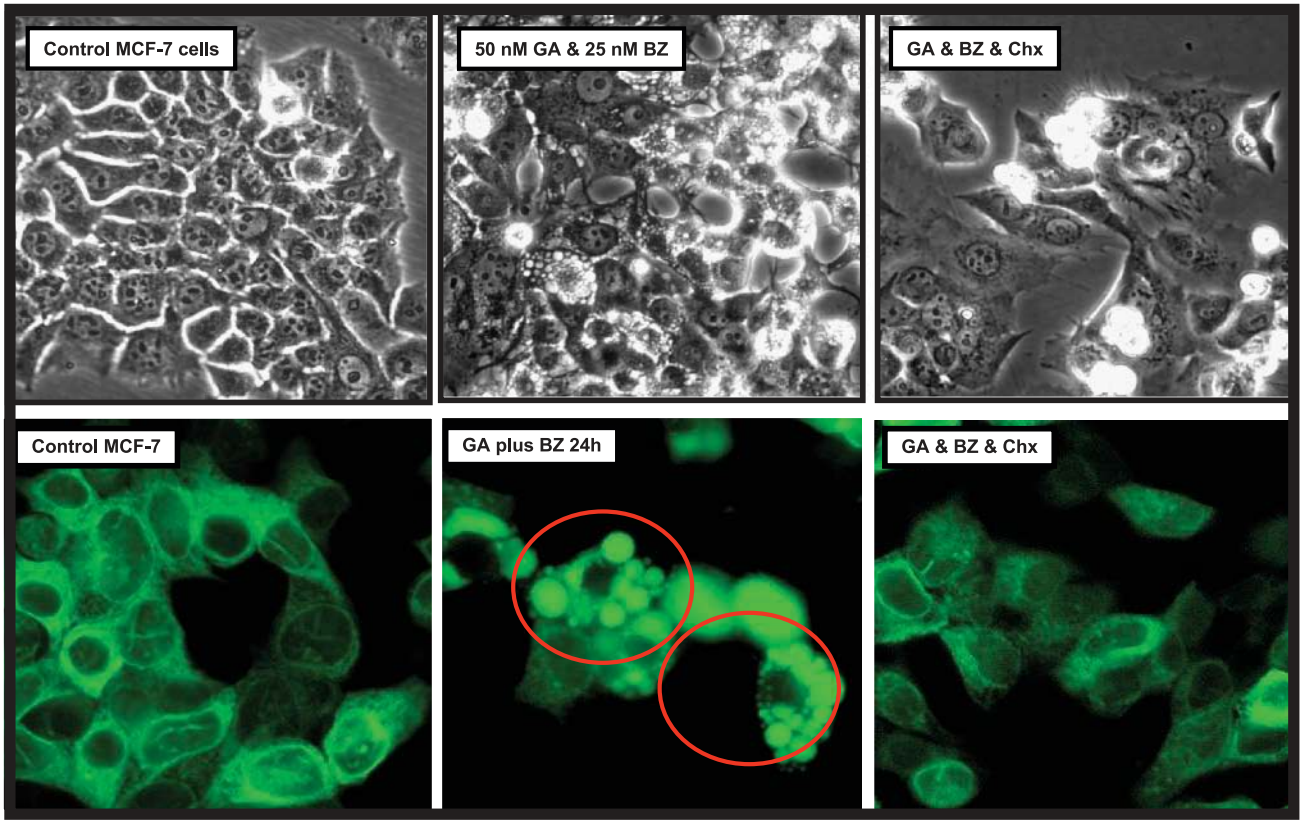

Figure 10. Cycloheximide blocks vacuolization in cells treated with geldanamycin and bortezomib. Tumor cells were incubated for 24 h with the indicated concentrations of geldanamycin and bortezomib alone or with 50 μg/ml cycloheximide to inhibit protein synthesis. The cells were visualized in the *top three panels* by phase contrast and the *bottom three panels* show the localization of the Living Colors ER marker that was detected with fluorescence microscopy. Note that in each case, cycloheximide completely prevented vacuolization of drug-treated cells, and the fluorescence of cells treated with geldanamycin and bortezomib plus cycloheximide resemble the control cells.

accumulation of ubiquitinated proteins and the enhanced antiproliferative activity of this two-drug combination, our data indicate a strong concordance between increased protein ubiquitination and drug combination-enhanced cytotoxicity. For example, geldanamycin plus bortezomib-induced ubiquitination and cytotoxicity were maximal when the two drugs were used simultaneously, they occurred at similarly low drug concentrations, and increased ubiquitination coincided temporally with the earliest signs of inhibition of proliferation.

As single agents, geldanamycin and bortezomib show selectivity against tumor cells compared with normal cell cohorts (20). One explanation for the tumor specificity of geldanamycin and 17-AAG is that these ansamycins destabilize and down-regulate many hsp 90-dependent mutated and/or constitutively active oncoproteins that drive proliferation and confer survival advantage to tumors (7, 67). Recently, Kamal *et al.* (68) offered an additional explanation for the relative antitumor selectivity of 17-AAG. They reported that tumor hsp 90, unlike normal cell hsp 90, adopts a conformation with elevated ATPase activity and high affinity for 17-AAG (68). Thus, tumor hsp 90, rather than normal tissue hsp 90, is the preferred target for 17-AAG.

An important determinant of the selectivity of bortezomib is the reliance of tumor cells on the ubiquitin and proteasome-dependent activation of NF-κB (69, 70). However, other consequences of proteasome inhibition such as unscheduled stabilization of wild-type p53 (71, 72) and the cell cycle inhibitors $p21^{WAF1}$ and $p27^{KIP1}$ (22, 73) are thought to contribute to the antitumor activity of bortezomib. It is also possible, as we have postulated here, that bortezomib-stabilized, insoluble, misfolded, and ubiquitinated proteins would become inherently cytotoxic.

Herein, we addressed the question of the tumor specificity of 17-AAG combined with bortezomib using untransformed 3T3 fibroblasts and 3T3 cells that stably express the HPV E6 and E7 oncogenic proteins. While 17-AAG plus bortezomib did not affect the viability of control fibroblasts, E6 and E7 oncoprotein-expressing cells were sensitized to the 17-AAG plus bortezomib combination. Although we recognize the shortcomings of this model system, it nevertheless does provide an opportunity to compare the relative activities of 17-AAG, bortezomib, and drug combination against nontransformed and transformed cells, which otherwise share an identical genotype.

These data support the tantalizing possibility that the combination of 17-AAG and bortezomib might retain or even amplify the tumor specificity characteristic of the individual drugs.

Geldanamycin has been shown previously to initiate both heat shock factor 1 (HSF-1)-dependent cytosolic (74, 75) and IRE1α-dependent ER stress responses (53, 76). The mechanism by which bortezomib activates cytosolic

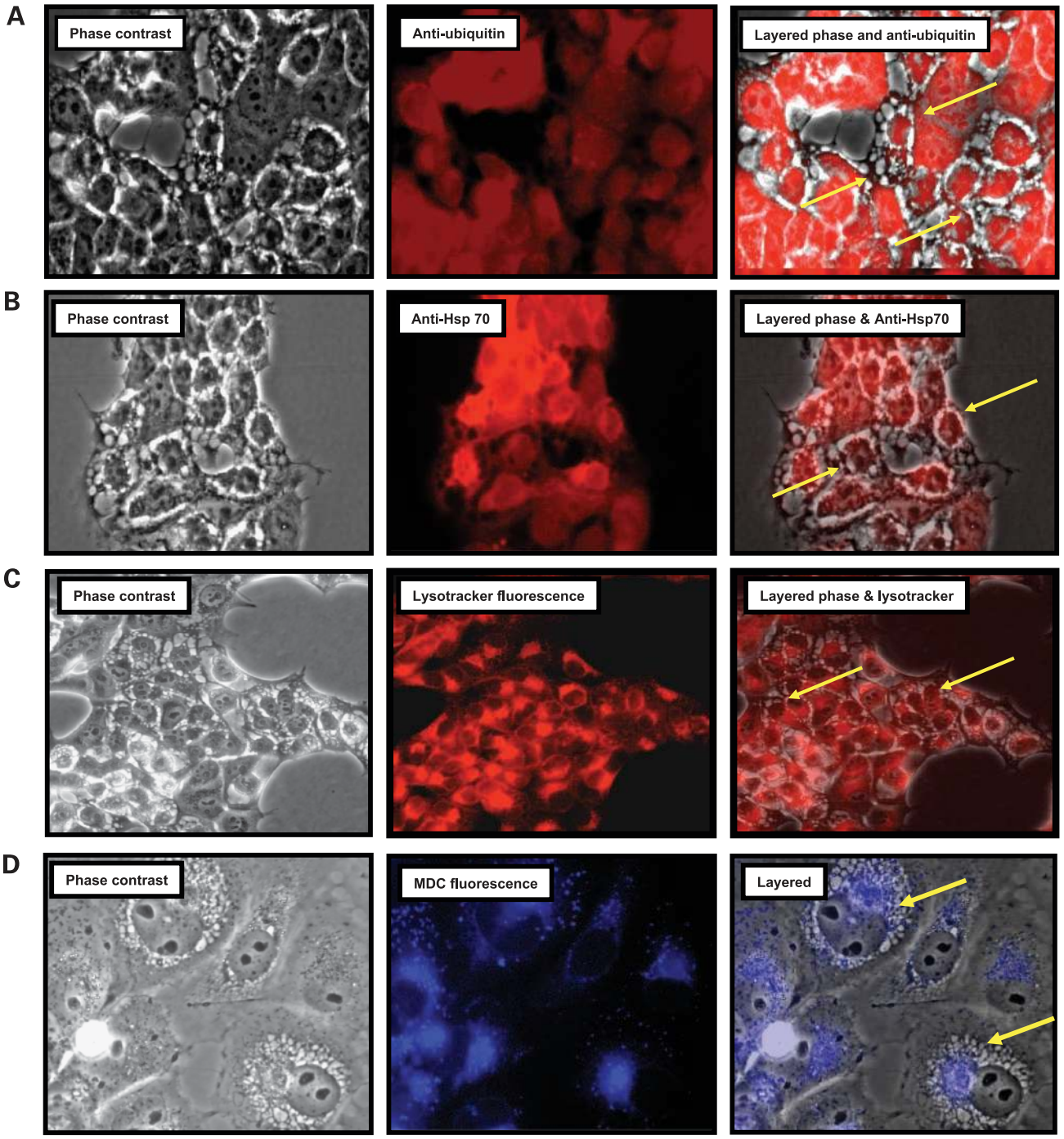

Figure 11. Immunofluorescence analysis of geldanamycin and bortezomib-induced vacuoles. Each *row of images* shows phase contrast, fluorescence, and layered phase contrast and fluorescence images of cells that had been treated with 50 nM geldanamycin and 25 nM bortezomib for 20 – 24 h. **A,** cells were probed with an anti-ubiquitin antibody. **B,** cells were probed with anti-hsp 70. **C,** cells were exposed to LysoTracker lysosomal fluorescent marker. **D,** cells were exposed to monodansylcadaverine, a fluorescent molecule that localizes in autophagosomes. Note that in all cases, the fluorescent probes remained outside the vacuoles (pointed out with *arrows* in the *right column of images*).

and ER stress responses is less clear, but inhibition of stress protein degradation may indirectly stabilize HSF-1 (77, 78), and proteasome inhibitors have been reported to activate HSF-2 (79). Moreover, proteasome inhibition interferes with retrograde transportation and degradation of misfolded proteins from within the ER compartment, thus triggering the ER stress response (80). Because both hsp 70 and hsp 90 accumulated in the detergent-insoluble fraction of cells exposed to geldanamycin plus bortezomib, these highly induced stress proteins were more than likely bound to aggregates of ubiquitinated cytosolic proteins. It is known that many hsp 90 client proteins aggregate and localize in the detergent-insoluble pellet fraction of cells treated with geldanamycin and a proteasome inhibitor (66, 81, 82). hsp 90 and hsp 70 stress proteins failed to localize in the detergent-insoluble fraction when cycloheximide blocked protein synthesis, and we also observed that cycloheximide completely prevented the increase in protein ubiquitination caused by geldanamycin plus bortezomib. These observations are consistent with the possibility that hsp 90 and hsp 70 relocated to an insoluble compartment in geldanamycin plus bortezomib-treated cells because they were associated with newly synthesized, ubiquitinated, and aggregated proteins. Induction of the ER-localized chaperone GRP78/BiP by geldanamycin plus bortezomib treatment indicates the unfolded protein response within that compartment had been activated. We propose that this powerful ER stress might be linked to the prodigious cell vacuolization that occurred in cells treated with this drug combination.

Exactly how does geldanamycin plus bortezomib induce the perinuclear vacuoles and what is their function? First, vacuolization was clearly hsp 90 dependent because several other hsp 90 inhibitors generated vacuoles when combined with bortezomib. Geldanamycin alone, even at high concentrations, could not promote vacuolization. Proteasome inhibition was also required, and other proteasome inhibitors were able to substitute for bortezomib in generating the vacuole phenotype, provided geldanamycin was also included. It is known that certain hsp 90 client proteins transit the ER Golgi network as they traffic to the plasma membrane. Thus, in geldanamycin-treated cells, newly synthesized ErbB2 fails to fold properly, does not undergo mature glycosylation, and is rapidly degraded by the ubiquitin-proteasome pathway (4, 6, 59). Misfolded ER proteins normally undergo retrograde translocation and proteolysis by a process termed ER-associated protein degradation. ER-associated protein degradation function requires ATP, ubiquitin, and proteasomes (83–85). In cells treated with bortezomib, geldanamycin-destabilized hsp 90 clients destined for the plasma membrane would likely accumulate within the ER because they could not be degraded by proteasomes. Thus, we suggest that geldanamycin plus bortezomib treatment not only promotes protein misfolding within the ER but also interferes with ER-associated protein degradation by preventing proteasome-linked retrograde translocation of those proteins across the ER membrane. Cells may respond to this situation by budding off ER membrane-bound vacuoles into the cytosol to relieve the misfolded protein blockade along the secretory pathway. Several of our observations support this hypothesis: First, vacuolization required inhibition of both hsp 90 and proteasomes. Second, geldanamycin plus bortezomib strongly induced the ER unfolded protein response in cells. Third, vacuoles were strongly positive for a fluorescent ER marker fusion protein, confirming their ER origin. Fourth, the vacuoles were negative for cytosolic proteins like ubiquitin and hsp 70. Fifth, cells cotreated with cycloheximide to shut off protein synthesis did not form vacuoles in the presence of geldanamycin plus bortezomib. Sixth, heat shock, which causes extensive protein misfolding (52), also induced the vacuolated phenotype in bortezomib-treated cells. Importantly, drug-induced vacuolization was reversible; when geldanamycin and bortezomib were washed from cells, the vacuoles diminished in size and disappeared within 24 h (data not shown). Taken together, these results indicate that geldanamycin plus bortezomib causes profound ER stress by interfering with ER-associated protein degradation and reversibly initiating remodeling of the ER membrane to form vacuoles. Geldanamycin plus bortezomib-induced ER vacuolization may represent a previously unappreciated defensive mechanism used by cells when proteasomes are incapable of participating in retrograde translocation of misfolded proteins out of the ER.

Given that geldanamycin and bortezomib exhibit significant specificity for tumor cells compared with normal tissue counterparts, one might speculate that a geldanamycin plus bortezomib regimen would have a favorable therapeutic index *in vivo*. Of course, the antitumor effectiveness of this drug combination *in vivo* will also be influenced by pharmacokinetic and tumor-dependent factors not addressed in this study, and the actual potency of geldanamycin plus bortezomib chemotherapy may vary depending on the particular type of cancer. For instance, at low nanomolar concentrations, bortezomib is effective against myeloma cells within 24 h (23), whereas bortezomib alone is only modestly effective against MCF-7 cells after several days of exposure. Therefore, geldanamycin plus bortezomib might be especially useful in treating multiple myeloma.

Although our study is predominantly mechanistic, it nevertheless provides a compelling rationale for pursuing the clinical development of a 17-AAG/bortezomib combination for treatment of multiple human malignancies.

References

1. Stebbins CE, Russo AA, Schneider C, Rosen N, Hartl FU, Pavletich NP. Crystal structure of an Hsp90-geldanamycin complex: targeting of a protein chaperone by an antitumor agent. Cell 1997;89:239–50.

2. Grenert JP, Sullivan WP, Fadden P, et al. The amino-terminal domain of heat shock protein 90 (hsp90) that binds geldanamycin is an ATP/ADP switch domain that regulates hsp90 conformation. J Biol Chem 1997;272:23843–50.

3. Prodromou C, Roe SM, O'Brien R, Ladbury JE, Piper PW, Pearl LH. Identification and structural characterization of the ATP/ADP-binding site in the Hsp90 molecular chaperone. Cell 1997;90:65–75.

4. Miller P, DiOrio C, Moyer M, et al. Depletion of the erbB-2 gene product p185 by benzoquinoid ansamycins. Cancer Res 1994;54:2724–30.

5. Whitesell L, Mimnaugh EG, DeCosta B, Myers CE, Neckers LM. Inhibition of heat shock protein HSP90-pp60$^{v\text{-}src}$ heteroprotein complex formation by benzoquinone ansamycins: essential role for stress proteins in oncogenic transformation. Proc Natl Acad Sci USA 1994;91:8324–8.

6. Mimnaugh EG, Chavany C, Neckers L. Polyubiquitination and proteasomal degradation of the p185c-erbB-2 receptor protein-tyrosine kinase induced by geldanamycin. J Biol Chem 1996;271:22796 – 801.

7. Neckers L, Schulte TW, Mimnaugh E. Geldanamycin as a potential anti-cancer agent: its molecular target and biochemical activity. Invest New Drugs 1999;17:361 – 73.

8. Neckers L, Neckers K. Heat-shock protein 90 inhibitors as novel cancer chemotherapeutic agents. Exp Opin Emerg Drugs 2002;7:277 – 88.

9. Maloney A, Workman P. HSP90 as a new therapeutic target for cancer therapy: the story unfolds. Exp Opin Biol Ther 2002;2:3 – 24.

10. Goetz MP, Toft DO, Ames MM, Erlichman C. The Hsp90 chaperone complex as a novel target for cancer therapy. Ann Oncol 2003;14:1169 – 76.

11. Supko JG, Hickman RL, Grever MR, Malspeis L. Preclinical pharmacologic evaluation of geldanamycin as an antitumor agent. Cancer Chemother Pharmacol 1995;36:305 – 15.

12. Neckers L. Development of small molecule hsp90 inhibitors: utilizing both forward and reverse chemical genomics for drug identification. Curr Med Chem 2003;10:733 – 9.

13. Sausville EA, Tomaszewski JE, Ivy P. Clinical development of 17-allylamino, 17-demethoxygeldanamycin. Curr Cancer Drug Targets 2003; 3:377 – 83.

14. Deshaies RJ. The self-destructive personality of a cell cycle in transition. Curr Opin Cell Biol 1995;7:781 – 9.

15. Pagano M. Cell cycle regulation by the ubiquitin pathway. FASEB J 1997;11:1067 – 75.

16. Desterro JM, Rodriguez MS, Hay RT. Regulation of transcription factors by protein degradation. Cell Mol Life Sci 2000;57:1207 – 19.

17. Bashir T, Pagano M. Aberrant ubiquitin-mediated proteolysis of cell cycle regulatory proteins and oncogenesis. Adv Cancer Res 2003;88: 101 – 44.

18. Teicher BA, Ara G, Herbst R, Palombella VJ, Adams J. The proteasome inhibitor PS-341 in cancer therapy. Clin Cancer Res 1999;5:2638 – 45.

19. Adams J, Palombella VJ, Sausville EA, et al. Proteasome inhibitors: a novel class of potent and effective antitumor agents. Cancer Res 1999; 59:2615 – 22.

20. Masdehors P, Omura S, Merle-Beral H, et al. Increased sensitivity of CLL-derived lymphocytes to apoptotic death activation by the proteasome-specific inhibitor lactacystin. Br J Haematol 1999;105: 752 – 7.

21. Drexler HC. Activation of the cell death program by inhibition of proteasome function. Proc Natl Acad Sci USA 1997;94:855 – 60.

22. Hideshima T, Richardson P, Chauhan D, et al. The proteasome inhibitor PS-341 inhibits growth, induces apoptosis, and overcomes drug resistance in human multiple myeloma cells. Cancer Res 2001;61:3071 – 6.

23. Adams J. Preclinical and clinical evaluation of proteasome inhibitor PS-341 for the treatment of cancer. Curr Opin Chem Biol 2002;6:493 – 500.

24. Wright JJ, Zerivitz K, Schoenfeldt M. Clinical trials referral resource. Current clinical trials of bortezomib. Oncology (Huntingt) 2003;17: 677 – 92.

25. Mitsiades N, Mitsiades CS, Poulaki V, et al. Molecular sequelae of proteasome inhibition in human multiple myeloma cells. Proc Natl Acad Sci USA 2002;99:14374 – 9.

26. Orlowski RZ, Stinchcombe TE, Mitchell BS, et al. Phase I trial of the proteasome inhibitor PS-341 in patients with refractory hematologic malignancies. J Clin Oncol 2002;20:4420 – 7.

27. Richardson PG, Barlogie B, Berenson J, et al. A phase 2 study of bortezomib in relapsed, refractory myeloma. N Engl J Med 2003;348: 2609 – 17.

28. Adams J. Potential for proteasome inhibition in the treatment of cancer. Drug Discov Today 2003;8:307 – 15.

29. Lenz HJ. Clinical update: proteasome inhibitors in solid tumors. Cancer Treat Rev 2003;29:41 – 8.

30. Adams J. Proteasome inhibition in cancer: development of PS-341. Semin Oncol 2001;28:613 – 9.

31. Rothwarf DM, Karin M. The NF-κB activation pathway: a paradigm in information transfer from membrane to nucleus. Sci STKE 1999; 1999:RE1.

32. Sunwoo JB, Chen Z, Dong G, et al. Novel proteasome inhibitor PS-341 inhibits activation of nuclear factor-κB, cell survival, tumor growth, and angiogenesis in squamous cell carcinoma. Clin Cancer Res 2001;7:1419 – 28.

33. Alkalay I, Yaron A, Hatzubai A, Orian A, Ciechanover A, Ben-Neriah Y. Stimulation-dependent IκBα phosphorylation marks the NF-κB inhibitor for degradation via the ubiquitin-proteasome pathway. Proc Natl Acad Sci USA 1995;92:10599 – 603.

34. Lin YC, Brown K, Siebenlist U. Activation of NF-κB requires proteolysis of the inhibitor IκB-α: signal-induced phosphorylation of IκB-α alone does not release active NF-κB. Proc Natl Acad Sci USA 1995;92:552 – 6.

35. Hershko A, Ciechanover A. The ubiquitin system. Annu Rev Biochem 1998;67:425 – 79.

36. Bonifacino JS, Weissman AM. Ubiquitin and the control of protein fate in the secretory and endocytic pathways. Annu Rev Cell Dev Biol 1998;14:19 – 57.

37. Mossman T. Rapid colormetric assay for cellular growth and survival: application to proliferation and cytotoxic assays. J Immunol Methods 1983;65:55 – 63.

38. Demers GW, Halbert CL, Galloway DA. Elevated wild-type p53 protein levels in human epithelial cell lines immortalized by the human papillomavirus type 16 E7 gene. Virology 1994;198:169 – 74.

39. Bradbury D, Bowen G, Kozlowski R, Reilly I, Russell N. Endogenous interleukin-1 can regulate the autonomous growth of the blast cells of acute myeloblastic leukemia by inducing autocrine secretion of GM-CSF. Leukemia 1990;4:44 – 7.

40. Lightcap ES, McCormack TA, Pien CS, Chau V, Adams J, Elliott PJ. Proteasome inhibition measurements: clinical application. Clin Chem 2000; 46:673 – 83.

41. Smith PK, Krohn RI, Hermanson GT, et al. BCA protein assay. Anal Biochem 1985;150:76 – 85.

42. Laemmli UK. Cleavage of structural proteins during the assembly of the head of bacteriophage T4. Nature (Lond) 1970;227:680 – 5.

43. Swerdlow PS, Finley D, Varshavsky A. Enhancement of immunoblot sensitivity by heating of hydrated filters. Anal Biochem 1986;156:147 – 53.

44. Bobrow MN, Harris TD, Shaughnessy KJ, Litt GJ. Catalyzed reporter disposition, a novel method of signal amplification. J Immunol Methods 1989;125:279 – 85.

45. Snedecor GW. Statistical methods. Ames, IA: Iowa State University Press; 1956. p. 45.

46. Demers GW, Foster SA, Halbert CL, Galloway DA. Growth arrest by induction of p53 in DNA damaged keratinocytes is bypassed by human papillomavirus 16 E7. Proc Natl Acad Sci USA 1994;91:4382 – 6.

47. Bedell MA, Jones KH, Grossman SR, Laimins LA. Identification of human papillomavirus type 18 transforming genes in immortalized and primary cells. J Virol 1989;63:1247 – 55.

48. Kaufmann WK, Schwartz JL, Hurt JC, et al. Inactivation of G_2 checkpoint function and chromosomal destabilization are linked in human fibroblasts expressing human papillomavirus type 16 E6. Cell Growth & Differ 1997;8:1105 – 14.

49. Xu W, Mimnaugh E, Rosser MF, et al. Sensitivity of mature Erbb2 to geldanamycin is conferred by its kinase domain and is mediated by the chaperone protein Hsp90. J Biol Chem 2001;276:3702 – 8.

50. Lindquist S. The heat-shock response. Annu Rev Biochem 1986;55: 1151 – 91.

51. Smith DF, Whitesell L, Katsanis E. Molecular chaperones: biology and prospects for pharmacological intervention. Pharmacol Rev 1998;50: 493 – 514.

52. Welch WJ. Heat shock proteins functioning as molecular chaperones: their roles in normal and stressed cells. Philos Trans R Soc Lond B Biol Sci 1993;339:327 – 33.

53. Lawson B, Brewer JW, Hendershot LM. Geldanamycin, an hsp90/GRP94-binding drug, induces increased transcription of endoplasmic reticulum (ER) chaperones via the ER stress pathway. J Cell Physiol 1998;174:170 – 8.

54. Winklhofer KF, Reintjes A, Hoener MC, Voellmy R, Tatzelt J. Geldanamycin restores a defective heat shock response *in vivo.* J Biol Chem 2001;276:45160 – 7.

55. Bush KT, Goldberg AL, Nigam SK. Proteasome inhibition leads to a heat-shock response, induction of endoplasmic reticulum chaperones and thermotolerance. J Biol Chem 1997;272:9086 – 92.

56. Kawazoe Y, Nakai A, Tanabe M, Nagata K. Proteasome inhibition leads to the activation of all members of the heat-shock-factor family. Eur J Biochem 1998;255:356 – 62.

57. Johnston JA, Ward CL, Kopito RR. Aggresomes: a cellular response to misfolded proteins. J Cell Biol 1998;143:1883 – 98.

58. Kopito RR. Aggresomes, inclusion bodies and protein aggregation. Trends Cell Biol 2000;10:524 – 30.

59. Chavany C, Mimnaugh E, Miller P, et al. p185erbB2 binds to GRP94 *in vivo.* Dissociation of the p185erbB2/GRP94 heterocomplex by benzoquinone ansamycins precedes depletion of p185erbB2. J Biol Chem 1996; 271:4974 – 7.

60. Wojcik C. An inhibitor of the chymotrypsin-like activity of the proteasome (PSI) induces similar morphological changes in various cell lines. Folia Histochem Cytobiol 1997;35:211 – 4.

61. Zhang Y, Nijbroek G, Sullivan ML, et al. Hsp70 molecular chaperone facilitates endoplasmic reticulum-associated protein degradation of cystic fibrosis transmembrane conductance regulator in yeast. Mol Biol Cell 2001;12:1303 – 14.

62. Neckers L, Mimnaugh EG, Schulte TW. The Hsp90 chaperone family. In: Latchman DS, editor. Stress proteins. Handbook of experimental pharmacology, vol. 136. Berlin: Springer-Verlag; 1999. p. 9 – 42.

63. Adams J. The proteasome: structure, function, and role in the cell. Cancer Treat Rev 2003;29:3 – 9.

64. Glickman MH, Ciechanover A. The ubiquitin-proteasome proteolytic pathway: destruction for the sake of construction. Physiol Rev 2002; 82:373 – 428.

65. Blagosklonny MV, Toretsky J, Neckers L. Geldanamycin selectively destabilizes and conformationally alters mutated p53. Oncogene 1995;11: 933 – 9.

66. Schulte TW, Blagosklonny MV, Ingui C, Neckers L. Disruption of the Raf-1-Hsp90 molecular complex results in destabilization of Raf-1 and loss of Raf-1-Ras association. J Biol Chem 1995;270: 24585 – 8.

67. Neckers L. Hsp90 inhibitors as novel cancer chemotherapeutic agents. Trends Mol Med 2002;8:S55 – 61.

68. Kamal A, Thao L, Sensintaffar J, et al. A high-affinity conformation of Hsp90 confers tumor selectivity on Hsp90 inhibitors. Nature 2003;425: 407 – 10.

69. Cusack JC Jr, Liu R, Houston M, et al. Enhanced chemosensitivity to CPT-11 with proteasome inhibitor PS-341: implications for systemic nuclear factor-κB inhibition. Cancer Res 2001;61:3535 – 40.

70. Adams J. Development of the proteasome inhibitor PS-341. Oncologist 2002;7:9 – 16.

71. Maki CG, Huibregtse JM, Howley PM. *In vivo* ubiquitination and proteasome-mediated degradation of p53(1). Cancer Res 1996;56: 2649 – 54.

72. Williams SA, McConkey DJ. The proteasome inhibitor bortezomib stabilizes a novel active form of p53 in human LNCaP-Pro5 prostate cancer cells. Cancer Res 2003;63:7338 – 44.

73. Pagano M, Tam SW, Theodoras AM, et al. Role of the ubiquitin-proteasome pathway in regulating abundance of the cyclin-dependent kinase inhibitor p27. Science 1995;269:682 – 5.

74. Bagatell R, Paine-Murrieta GD, Taylor CW, et al. Induction of a heat shock factor 1-dependent stress response alters the cytotoxic activity of hsp90-binding agents. Clin Cancer Res 2000;6: 3312 – 8.

75. Knowlton AA, Sun L. Heat-shock factor-1, steroid hormones, and regulation of heat-shock protein expression in the heart. Am J Physiol Heart Circ Physiol 2001;280:H455 – 64.

76. Marcu MG, Doyle M, Bertolotti A, Ron D, Hendershot L, Neckers L. Heat shock protein 90 modulates the unfolded protein response by stabilizing IRE1α. Mol Cell Biol 2002;22:8506 – 13.

77. Kim D, Kim SH, Li GC. Proteasome inhibitors MG132 and lactacystin hyperphosphorylate HSF1 and induce hsp70 and hsp27 expression. Biochem Biophys Res Commun 1999;254:264 – 8.

78. Pirkkala L, Alastalo TP, Zuo X, Benjamin IJ, Sistonen L. Disruption of heat shock factor 1 reveals an essential role in the ubiquitin proteolytic pathway. Mol Cell Biol 2000;20:2670 – 5.

79. Mathew A, Mathur SK, Morimoto RI. Heat shock response and protein degradation: regulation of HSF2 by the ubiquitin-proteasome pathway. Mol Cell Biol 1998;18:5091 – 8.

80. Kostova Z, Wolf DH. For whom the bell tolls: protein quality control of the endoplasmic reticulum and the ubiquitin-proteasome connection. EMBO J 2003;22:2309 – 17.

81. An WG, Schulte TW, Neckers LM. The heat shock protein 90 antagonist geldanamycin alters chaperone association with p210bcr-abl and v-src proteins before their degradation by the proteasome. Cell Growth & Differ 2000;11:355 – 60.

82. Basso AD, Solit DB, Chiosis G, Giri B, Tsichlis P, Rosen N. Akt forms an intracellular complex with heat shock protein 90 (Hsp90) and Cdc37 and is destabilized by inhibitors of Hsp90 function. J Biol Chem 2002; 277:39858 – 66.

83. Plemper RK, Wolf DH. Retrograde protein translocation: ERADication of secretory proteins in health and disease. Trends Biochem Sci 1999; 24:266 – 70.

84. Ye Y, Meyer HH, Rapoport TA. Function of the p97-Ufd1-Npl4 complex in retrotranslocation from the ER to the cytosol: dual recognition of nonubiquitinated polypeptide segments and polyubiquitin chains. J Cell Biol 2003;162:71 – 84.

85. Jarosch E, Lenk U, Sommer T. Endoplasmic reticulum-associated protein degradation. Int Rev Cytol 2003;223:39 – 81.